International Journal of Pharmacology

Int. J. Pharmacol. **2026**; 22(5): 53817
https://doi.org/10.31083/IJP53817

Research Article

Hesperidin Enhances the Antitumor Effect of Gefitinib Against Non-Small Cell Lung Cancer via Activation of Endoplasmic Reticulum Stress

Juan Pan[1,2], Youjing Wang[3], Tingting Li[4], Yangyang Lü[4], Jia Yi[2], Dan Liu[1,2,*]

[1]Department of Basic Medicine, Chongqing Three Gorges Medical College, 404120 Chongqing, China
[2]Chongqing Key Laboratory of Development and Utilization of Genuine Medicinal Materials in Three Gorges Reservoir Area, 404120 Chongqing, China
[3]Major in Biological and Pharmaceutical Engineering, School of Life Sciences, Yunnan University, 650000 Kunming, Yunnan, China
[4]Major in Bioengineering, College of Modern Agriculture and Bioengineering, Yangtze Normal University, 408000 Chongqing, China
*Correspondence: 20130203@cqtgmc.edu.cn (Dan Liu)
Academic Editor: Mehmet Ozaslan
Submitted: 13 May 2026 Revised: 1 August 2026 Accepted: 3 August 2026 Published: 16 September 2026

Abstract

Background: This study was designed to evaluate whether hesperidin (HES) could enhance the antitumor activity of gefitinib (GEF) against A549 non-small cell lung cancer (NSCLC) cells. Moreover, the molecular basis of this activity was also investigated using both *in vitro* and *in vivo* approaches. **Methods:** The viability of A549 cells treated with HES and GEF, alone or in combination, was assessed using the Cell Counting Kit-8 (CCK-8) assay to determine half-maximal inhibitory concentrations (IC_{50}) and the suitable combination ratio. Cell morphology, migratory capacity, and apoptosis were examined by light microscopy, wound-healing assay, and flow cytometry, respectively. Expression levels of endoplasmic reticulum stress-related proteins, including ATF4 (activating transcription factor 4) and CHOP (C/EBP homologous protein), as well as cleaved caspase-3 were evaluated by Western blotting. An A549 xenograft model was established in nude mice to validate the antitumor efficacy and systemic safety of HES and GEF *in vivo*. **Results:** The IC_{50} values for HES and GEF in A549 cells were 153.1 μM and 30.28 μM, respectively. Compared with monotherapy, the HES/GEF combination induced pronounced morphological alterations, suppressed cell migration, and promoted apoptosis. This enhanced antitumor effect was associated with upregulation of ATF4, CHOP, and cleaved caspase-3 expression. In the xenograft model, combination therapy produced synergistic inhibition of tumor growth without inducing significant changes in body weight or major organ indices, indicating a favorable safety profile. **Conclusion:** HES synergizes with GEF to inhibit the malignant progression of A549 NSCLC cells, both *in vitro* and *in vivo*. The underlying mechanism may involve activation of endoplasmic reticulum stress-mediated apoptotic pathways.

Keywords: non-small cell lung cancer; hesperidin; gefitinib; apoptosis; endoplasmic reticulum stress

1. Introduction

Lung cancer is the most frequently diagnosed malignancy worldwide and the leading cause of cancer-related mortality [1]. Histologically, it is broadly classified into two major subtypes: non-small cell lung cancer (NSCLC), which accounts for approximately 85% of all cases, and small-cell lung cancer (SCLC), comprising the remaining 15% [2]. Despite its high incidence, the five-year survival rate for lung cancer remains only about 19%, reflecting a generally poor prognosis [3].

Receptor tyrosine kinases (RTKs) are transmembrane glycoproteins that play pivotal roles in tumorigenesis by phosphorylating downstream substrates and activating cascades such as phosphatidylinositol 3-kinase (PI3K)/protein kinase B (AKT), rat sarcoma (RAS)/mitogen-activated protein kinase (MAPK), and Janus kinase (JAK)/signal transducer and activator of transcription (STAT). In NSCLC, key RTKs including epidermal growth factor receptor (EGFR), human epidermal growth factor receptor 2 (HER2), mesenchymal-epithelial transition factor (c-MET), anaplastic lymphoma kinase (ALK), and ROS proto-oncogene 1, receptor tyrosine kinase (ROS1) are frequently dysregulated through mutation, amplification, or chromosomal rearrangement, thereby driving oncogenic addiction and malignant progression [4,5]. Tyrosine kinase inhibitors (TKIs) that target these aberrant kinases have revolutionized NSCLC treatment. Gefitinib (GEF) is an EGFR-TKI that has proven effective for treating advanced NSCLC harboring EGFR-sensitive mutations [6]. Activating EGFR mutations, particularly exon 19 deletions and the L858R point mutation in exon 21, confer heightened sensitivity to EGFR-TKIs by stabilizing the active kinase conformation and enhancing ATP affinity [7,8].

However, a substantial proportion of NSCLC patients, particularly those with Kirsten rat sarcoma viral oncogene homolog (KRAS) mutations, exhibit intrinsic resistance to EGFR-TKIs, resulting in limited clinical benefit. Emerging evidence suggests that combining natural products with TKIs may overcome lung cancer resistance. There is growing research interest in the application of plant-derived

bioactive compounds as TKI sensitizers and modulators of signaling pathways [9]. Accordingly, investigation of combination strategies capable of enhancing GEF sensitivity, especially in the context of intrinsic resistance, may be of considerable value for optimizing therapeutic approaches in NSCLC.

Hesperidin (HES) is a flavonoid compound found in abundance in plants of the Rutaceae family such as limes and sweet oranges. It possesses diverse pharmacological properties, including anti-inflammatory [10,11], antioxidant [12], and anti-apoptotic effects [13], as well as beneficial roles in the treatment of diabetes and diabetic neuropathy [14], cardioprotection [15], and neuroprotection [16]. In recent years, increasing evidence has shown that HES possesses antitumor activity in various malignancies. It modulates multiple signaling pathways that influence the proliferation and apoptosis of different cancer cell types, including neuroblastoma, hepatocellular carcinoma, lung cancer, and colorectal cancer [17,18].

The endoplasmic reticulum (ER) is a central organelle for protein folding and quality control. When perturbed by hypoxia, nutrient deprivation, or protein misfolding, ER stress (ERS) triggers the unfolded protein response (UPR), which is mainly mediated by three sensors—inositol-requiring enzyme 1 (IRE1), activating transcription factor 6 (ATF6), and protein kinase RNA-like endoplasmic reticulum kinase (PERK)—that relay signals to re-establish ER balance. However, persistent or excessive ERS can induce apoptosis by UPR-mediated pathways. ERS and its associated UPR play complex and critical roles in the occurrence and progression of NSCLC, being deeply involved in multiple biological processes including the regulation of tumor cell apoptosis, autophagy, survival, proliferation, and drug resistance. Notably, the value of ERS in cancer treatment is becoming increasingly prominent. For example, the ursolic acid derivative UA232 (a synthetic derivative of ursolic acid) was reported to induce apoptosis in lung cancer cells through activation of the PERK/eukaryotic initiation factor 2α (eIF2α)/C/EBP homologous protein (CHOP) axis [19]. Similarly, Im et al. [20] demonstrated that Cytochrome b5 reductase 3 exerts tumor-suppressive effects by activating the PERK-activating transcription factor 4 (ATF4) and inositol-requiring enzyme 1α (IRE1α)-c-Jun N-terminal kinase (JNK) ERS pathways. The natural compound Flemiphilippinin A was recently found to trigger paraptosis in lung cancer cells by inducing excessive ERS and CHOP-mediated mitochondrial dysfunction. Moreover, low-dose Flemiphilippinin A in combination with GEF restored drug sensitivity in GEF-resistant cells [21]. These findings support the use of natural compounds targeting ERS to overcome EGFR-TKI resistance.

Consistently, a recent study have also found that hesperetin induces apoptosis in lung squamous carcinoma cells by activating ERS through G2/M phase arrest and Notch1 pathway inhibition, while exhibiting good safety profiles *in vivo* [22]. This study suggests that flavonoids, represented by hesperetin, may exert antitumor effects through the modulation of ERS pathways.

However, studies on the therapeutic effects and molecular mechanisms of the combined use of HES and EGFR-TKIs such as GEF in NSCLC remain limited, and it remains unclear whether HES enhances the antitumor efficacy of GEF via activation of the ERS pathway. The human NSCLC A549 cell line, which harbors wild-type EGFR and KRAS mutations, is intrinsically resistant to GEF and thus serves as an appropriate model for evaluating chemosensitization strategies [23]. The aim of this study was therefore to investigate the effects of HES alone and in combination with GEF on the proliferation, migration, and apoptosis of A549 cells. We also investigated whether the potential mechanism of these effects involved ERS and its related signaling pathways. The findings are expected to provide experimental and theoretical evidence for the potential application of HES/GEF combination therapy in NSCLC, as well as offering new insights into the development of low-toxicity and high-efficiency treatment strategies based on natural compounds.

2. Materials and Methods

2.1 Chemicals and Reagents

GEF (HPLC ≥98%; CAS No.184475-35-2), HES (HPLC ≥98%; CAS No.520-26-3), and sodium carboxymethyl cellulose (CMC-Na, CAS No.9004-32-4) were purchased from Shanghai Yuanye Bio-Technology Co., Ltd. (Shanghai, China). Fetal bovine serum (FBS, catalog 10099-141) and DMEM (catalog C11995500BT) were obtained from Gibco (Grand Island, NY, USA). The Cell Counting Kit-8 (CCK-8, catalog CA1210) was purchased from Beijing Solarbio Science & Technology Co., Ltd. (Beijing, China). ATF4 (catalog sc-390063) and CHOP (catalog sc-166682) antibodies were purchased from Santa Cruz Biotechnology, Inc. (Dallas, TX, USA), cleaved caspase-3 antibody (catalog AF7022) from Affinity Biosciences (Changzhou, China), and β-actin antibody (catalog F210074) from Abways Technology Co., Ltd. (Shanghai, China).

2.2 Instruments and Equipment

The microplate reader (model DNM-9602) was purchased from Beijing Pulang New Technology Co., Ltd. (Beijing, China); the inverted microscopy imaging system (model DMI8) from Leica (Wetzlar, Germany); the clinical-grade three-laser flow cytometer (model DXFlex) from Beckman Coulter (Brea, CA, USA); and the Western blot detection and analysis system (model 1704150) from Bio-Rad (Hercules, CA, USA).

2.3 Software and Data Analysis

Western blot images were acquired and analyzed using Image Lab Software (RRID:SCR_014210; Bio-Rad

Laboratories, Inc., Hercules, CA, USA; https://www.bio-rad.com/zh-cn/product/image-lab-software). All statistical analyses and graphical presentations were performed using GraphPad Prism 5 (RRID:SCR_002798; GraphPad Software, Inc., La Jolla, CA, USA; https://www.graphpad.com).

2.4 Cell Line and Experimental Animals

The human NSCLC cell line A549 was purchased from IMMOCELL (Xiamen Yimo Biotechnology Co., Ltd., Xiamen, Fujian, China; catalogue No. IM-H113). Five-week-old specific pathogen-free (SPF)-grade male BALB/c nude mice (n = 24) were purchased from Hunan Silaike Jingda Laboratory Animal Co., Ltd., License No. SCXK (Xiang) 2019-0004. All animal experiments were performed in the Animal Experimental Center of Chongqing Three Gorges Medical College. The study was approved by the Medical Ethics Committee of the college (Approval No. SXYZ-A-2404-0011) and carried out in accordance with the National Institutes of Health (NIH) Guide for the Care and Use of Laboratory Animals and the ARRIVE guidelines. During experiments, animals were maintained under SPF conditions at a controlled temperature (26–28 °C) and relative humidity (40–60%), with sterilized food, water, and bedding. The A549 cell line was validated by short tandem repeat (STR) profiling and tested negative for mycoplasma. A549 cells were cultured in DMEM supplemented with 10% FBS and 1% penicillin/streptomycin at 37 °C in a humidified atmosphere containing 5% CO_2. Cells between passages 6–14 were used.

2.5 Cell Viability and IC_{50} Determination by CCK-8 Assay

Logarithmic-phase A549 cells were trypsinized, counted, and seeded into 96-well plates at a density of 5 × 10^3 cells per well in 100 µL of medium, with six technical replicates per group. After 24 h of culture, the cells were exposed to graded concentrations of GEF (0, 5, 10, 20, 40, 50 µM) or HES (0, 20, 40, 80, 120, 160, 200 µM) for 48 h. Subsequently, 10 µL of CCK-8 solution was added to each well and incubated for 1–4 h. Absorbance was read at 450 nm using a microplate reader, and both the cell proliferation rate and IC_{50} values were subsequently calculated. IC_{50} values were determined by nonlinear regression, and the zero concentration control point was excluded from the fitting. The CCK-8 assay indirectly assesses cell viability by measuring metabolic activity. To determine whether the observed reduction in cell viability reflected decreased proliferation and/or increased apoptosis, flow cytometric analysis of Annexin V-fluorescein isothiocyanate/propidium iodide (Annexin V-FITC/PI) staining was performed in parallel.

2.6 Wound Healing Assay for Cell Migration

A549 cells were seeded into six-well plates and grown to 90% confluence. A linear scratch was created with a sterile 200 µL pipette tip, and detached cells were removed by three washes with PBS. Subsequently, the cells were treated with medium containing GEF, HES, and GEF+HES. Wound closure was monitored by the capture and analysis of images at 0, 24, and 48 h under an inverted microscope.

2.7 Flow Cytometry for the Detection of Apoptosis

To distinguish between cytostasis and apoptosis, apoptosis was quantified by flow cytometry. A549 cells were seeded in six-well plates and cultured for 24 h, followed by treatment with GEF, HES, or both for 48 h. Cells were then trypsinized without EDTA and centrifuged at 1000 rpm for 5 min. The supernatant was removed, and the cell pellet was washed with 1 mL of precooled PBS and centrifuged again. The resulting pellet was resuspended in 1× Binding Buffer to a density of 1–5 × 10^6 cells/mL. Subsequently, 100 µL of the cell suspension was transferred to new tubes, mixed with 5 µL Annexin V-FITC, and incubated for 5 min at room temperature in the dark, followed by the addition of 5 µL PI and 400 µL PBS. Samples were immediately analyzed by flow cytometry. Quadrants were defined as: Q1-UL (necrotic/damaged), Q1-UR (late apoptotic), Q1-LL (viable), and Q1-LR (early apoptotic). The apoptotic rate was calculated as the sum of Q1-UR and Q1-LR.

2.8 Western Blot Analysis

After 48 h of treatment, cells were collected, washed three times with PBS, and lysed on ice for 10–15 min. The lysate was centrifuged, and the supernatant was collected as total protein. Protein samples were mixed with loading buffer, denatured in a metal bath, and stored at –20 °C. Equal protein amounts were separated by sodium dodecyl sulfate–polyacrylamide gel electrophoresis (SDS-PAGE), transferred onto polyvinylidene difluoride (PVDF) membranes, and blocked with 5% skim milk for 2 h. Membranes were incubated overnight at 4 °C with primary antibodies against ATF4 (1:100 dilution), CHOP (1:100), cleaved caspase-3 (1:1000), and β-actin (1:6000). After washing with Tris-buffered saline with Tween 20 (TBST), the membranes were incubated with appropriate secondary antibodies for 2 h at room temperature. Protein bands were detected using ECL and quantified with Image Lab software.

2.9 Establishment of Xenograft Tumor Model and In Vivo Antitumor Evaluation

Five-week-old male nude mice (n = 24) were subcutaneously injected in the right hind leg with a suspension of 6 × 10^6 A549 cells in PBS. When the tumors became measurable, mice were randomly divided into four groups (n = 6 per group): Control, GEF (50 mg/kg), HES (100 mg/kg), and GEF + HES (50 + 100 mg/kg). The doses of GEF and HES were selected based on previous *in vivo* studies demonstrating antitumor efficacy without significant toxicity, as well as our preliminary dose-finding experiments

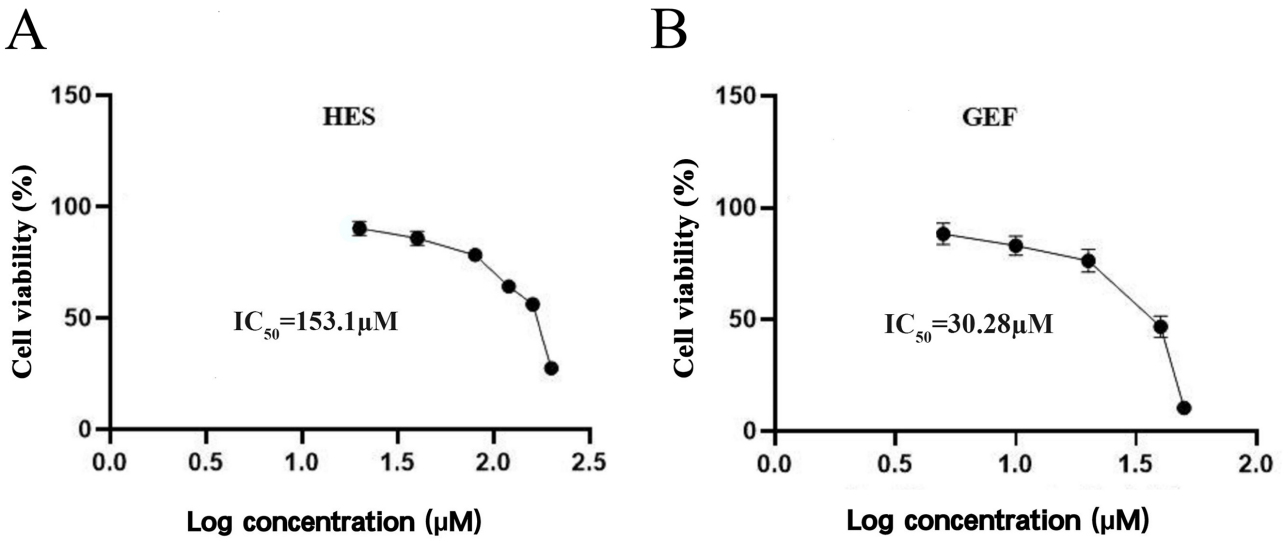

Fig. 1. Determination of the half-maximal inhibitory concentration (IC_{50}) of HES and GEF against A549 lung adenocarcinoma cells. Data are presented as the mean ± SD (n = 3 independent experiments). (A) Dose-response curve for HES (0–200 μM), with a fitted IC_{50} value of 153.1 μM. (B) Dose–response curve for GEF (0–50 μM), with a fitted IC_{50} value of 30.28 μM. HES, hesperidin; GEF, gefitinib.

[18,24]. Treatments were administered via oral gavage every two days. Tumor volume and body weight were measured on days 0, 4, 7, 10, 13, and 16. On day 16, following the final measurements, the mice were euthanized by intraperitoneal injection of 1% pentobarbital sodium at a dose of 200 mg/kg (10 mg/mL solution), and the tumors were excised and weighed. Tumor volume was calculated as: V (mm^3) = $width^2$ (mm) × length (mm) / 2.

2.10 Statistical Analysis

Data were analyzed with GraphPad Prism 5 using one-way ANOVA followed by Tukey's post-hoc test for multiple comparisons. All *in vitro* experiments were performed with three independent biological replicates (n = 3), each comprising three technical replicates. *In vivo* experiments included six mice per group (n = 6). Results are presented as the mean ± SD, with statistical significance defined as $p < 0.05$.

3. Results

3.1 Effects of GEF and HES Alone on A549 Cell Proliferation and IC_{50} Determination

CCK-8 assays were used to assess cell viability after 48 h treatment with varying concentrations of HES (0, 20, 40, 80, 120, 160, 200 μM) or GEF (0, 5, 10, 20, 40, 50 μM). The IC_{50} values were 153.1 μM for HES and 30.28 μM for GEF. Based on these results, concentrations of 35 μM HES and 15 μM GEF were chosen for subsequent combination experiments (Fig. 1A,B).

3.2 Effects of the HES and GEF Combination on Cell Morphology

After 24 h of treatment, both GEF and HES alone caused noticeable changes in A549 cell morphology compared with the control group, including increased intercellular spacing. The GEF + HES combination treatment further reduced cell numbers and markedly enlarged the gaps between cells, indicating a more pronounced effect on cell morphology (Fig. 2).

3.3 Effects of the HES and GEF Combination on Cell Migration

Wound-healing assays demonstrated that after treatment with GEF, HES, or GEF + HES at 0 h, 24 h, and 48 h, the migration of A549 cells was significantly inhibited in all treatment groups compared with the control, with the combination group showing the most pronounced inhibition. The wound area in the combination group remained widest at both 24 and 48 h, suggesting an enhanced suppression of A549 cell migration by HES and GEF (Fig. 3A,B).

3.4 Effects of the HES and GEF Combination on Apoptosis

Flow cytometric analysis revealed that all treatment groups showed significantly increased apoptosis rates compared with the control group. The combination group exhibited the highest apoptotic rate, indicating that co-treatment with HES and GEF promotes apoptosis in A549 cells (Fig. 4A,B).

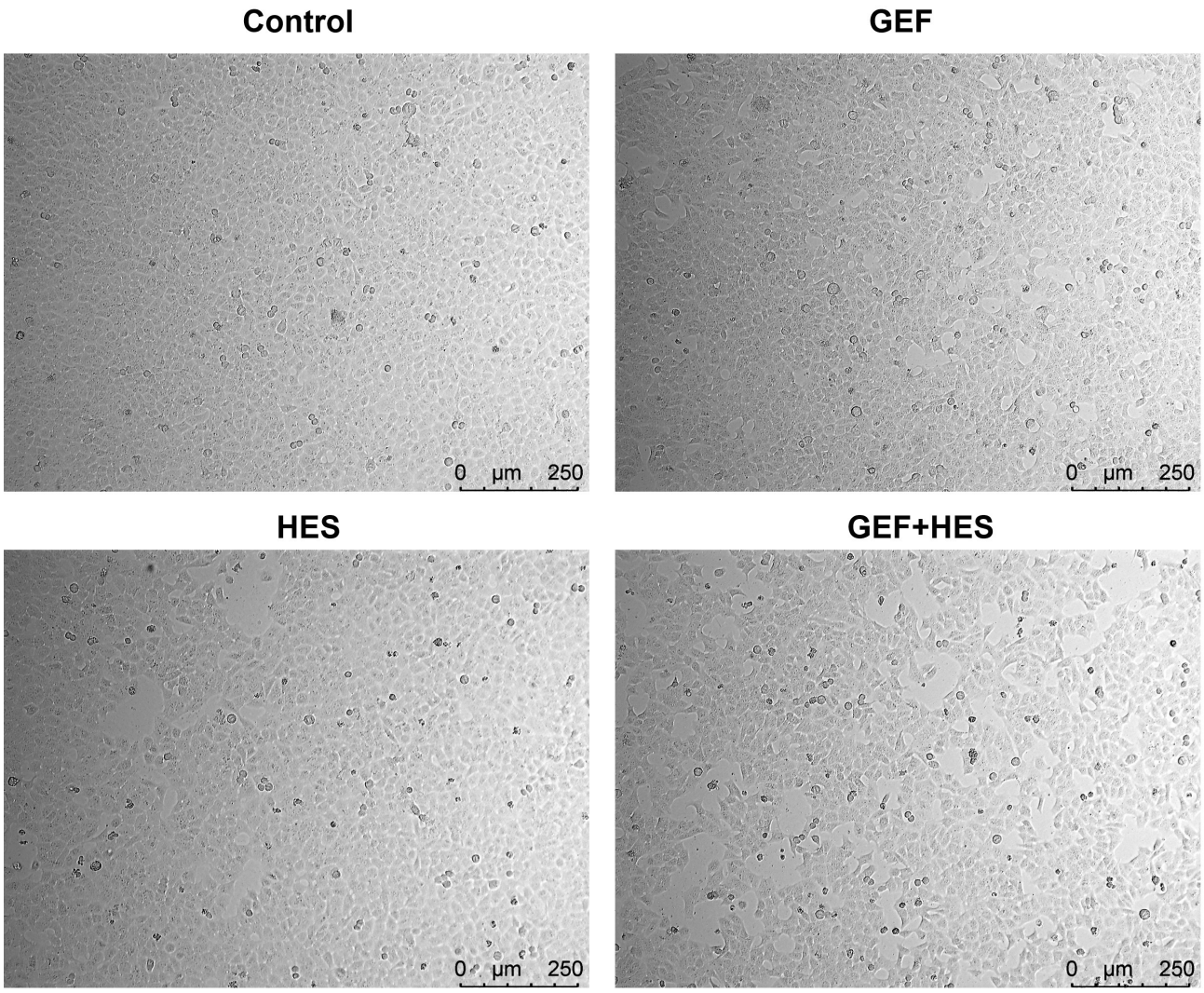

Fig. 2. Morphology of A549 cells after 24 h treatment with different drug concentrations (microscopic observation at 200× magnification). Control cells were dense and were in close contact. GEF (15 μM) alone increased intercellular spaces and reduced density, with HES (35 μM) alone showing similar changes. The GEF + HES (15 μM+35 μM) combination further reduced cell numbers and widened the intercellular gaps. Scale bar = 250 μm.

3.5 Expression of Key Proteins Detected by Western Blotting

Compared with the control group, combination treatment significantly increased the expression levels of the apoptosis-related protein cleaved caspase-3 and the ERS-related proteins ATF4 and CHOP, suggesting the drug combination may promote apoptosis through ERS pathways (Fig. 5A–D).

3.6 In Vivo Antitumor Efficacy of the HES and GEF Combination in Nude Mice

To further evaluate the *in vivo* antitumor efficacy of HES and GEF, a xenograft model with A549 cells was established in nude mice. Both HES and GEF alone inhibited tumor growth (volume and weight) compared with the control group, while the combination group exhibited the strongest inhibitory effect (Fig. 6A–D). During treatment, no significant differences were observed in body weight or major organ indices (heart, liver, spleen, lung, kidney), indicating an acceptable preliminary safety profile at the tested doses based on body weight and organ indices (Fig. 6E).

4. Discussion

Flavonoids are a class of naturally occurring bioactive compounds widely present in fruits and vegetables. They have demonstrated considerable potential in cancer prevention and therapy, acting through multiple mechanisms to effectively inhibit tumorigenesis and cancer cell proliferation [25]. In recent years, combination therapy has increasingly become a focal point in oncology research. The integration of conventional anticancer agents with low-toxicity natural

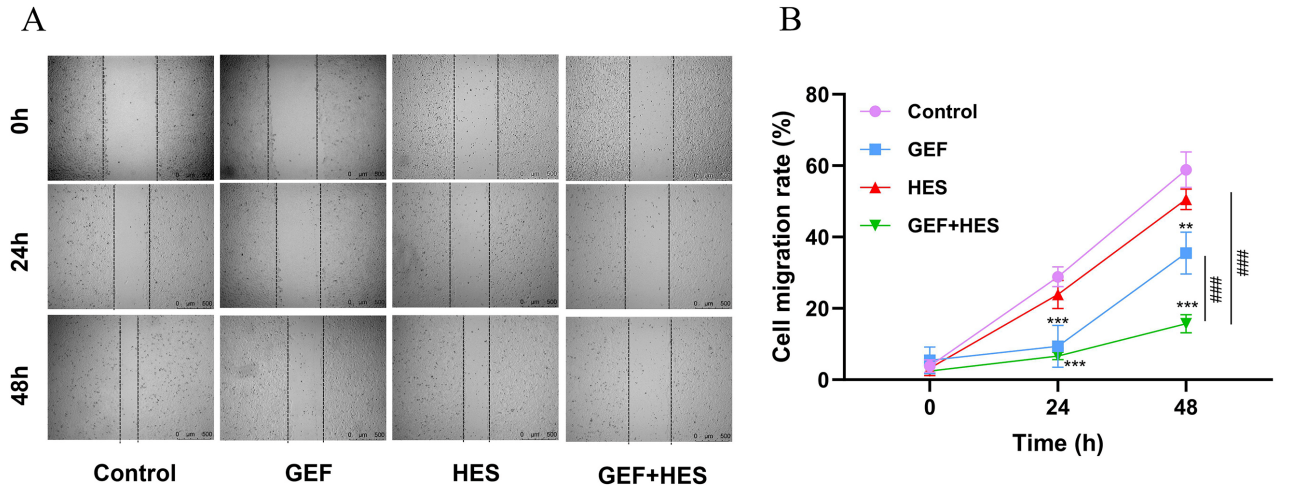

Fig. 3. Inhibition of A549 cell migration by HES and GEF. (A) Representative wound healing images at 0, 24, and 48 h after treatment with control, GEF, HES, and GEF + HES. (B) Quantitative analysis of wound closure (expressed as migration rate) at the indicated time points. Data are shown as the mean ± SD (n = 3). Compared with the control group, $^{**}p < 0.01$, $^{***}p < 0.001$; compared with the single drug group, $^{###}p < 0.001$. Scale bar = 500 μm.

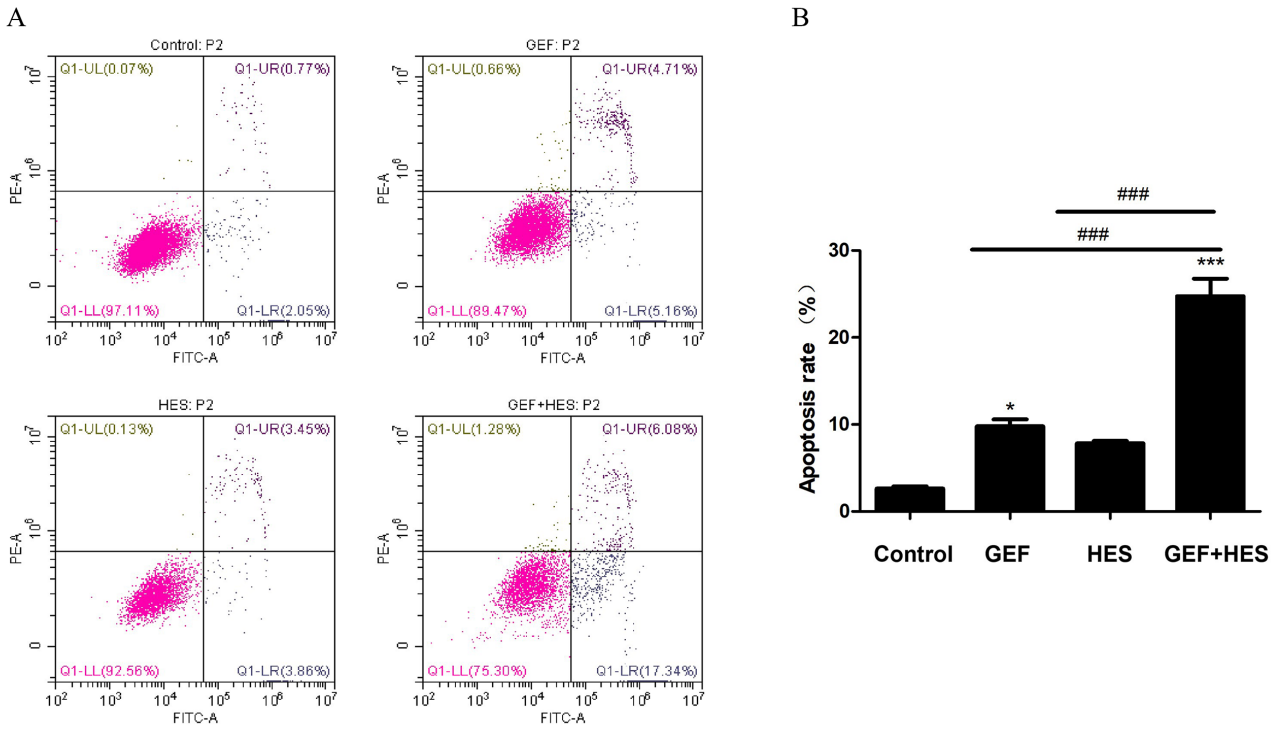

Fig. 4. Induction of apoptosis in A549 cells by HES and GEF. (A) Representative flow cytometry dot plots of Annexin V-FITC/PI double staining after 48 h treatment with control, GEF, HES, and GEF + HES. Quadrants indicate viable (lower left), early apoptotic (lower right), late apoptotic (upper right), and necrotic (upper left) cells. (B) Quantitative analysis of total apoptosis rates (early + late apoptotic cells) for each group. Data are shown as the mean ± SD (n = 3). $^{*}p < 0.05$, $^{***}p < 0.001$ compared to the control group; $^{###}p < 0.001$ compared to the single-drug group. Annexin V-FITC/PI, Annexin V-fluorescein isothiocyanate/propidium iodide.

bioactive components offers the prospect of synergistic action via multiple pathways, thereby overcoming resistance to monotherapy and improving the overall therapeutic outcomes [26,27].

In this study, we investigated the enhanced antitumor effect of the flavonoid HES in combination with GEF in the NSCLC A549 cell model. *In vitro* experiments demonstrated that, compared with either agent alone,

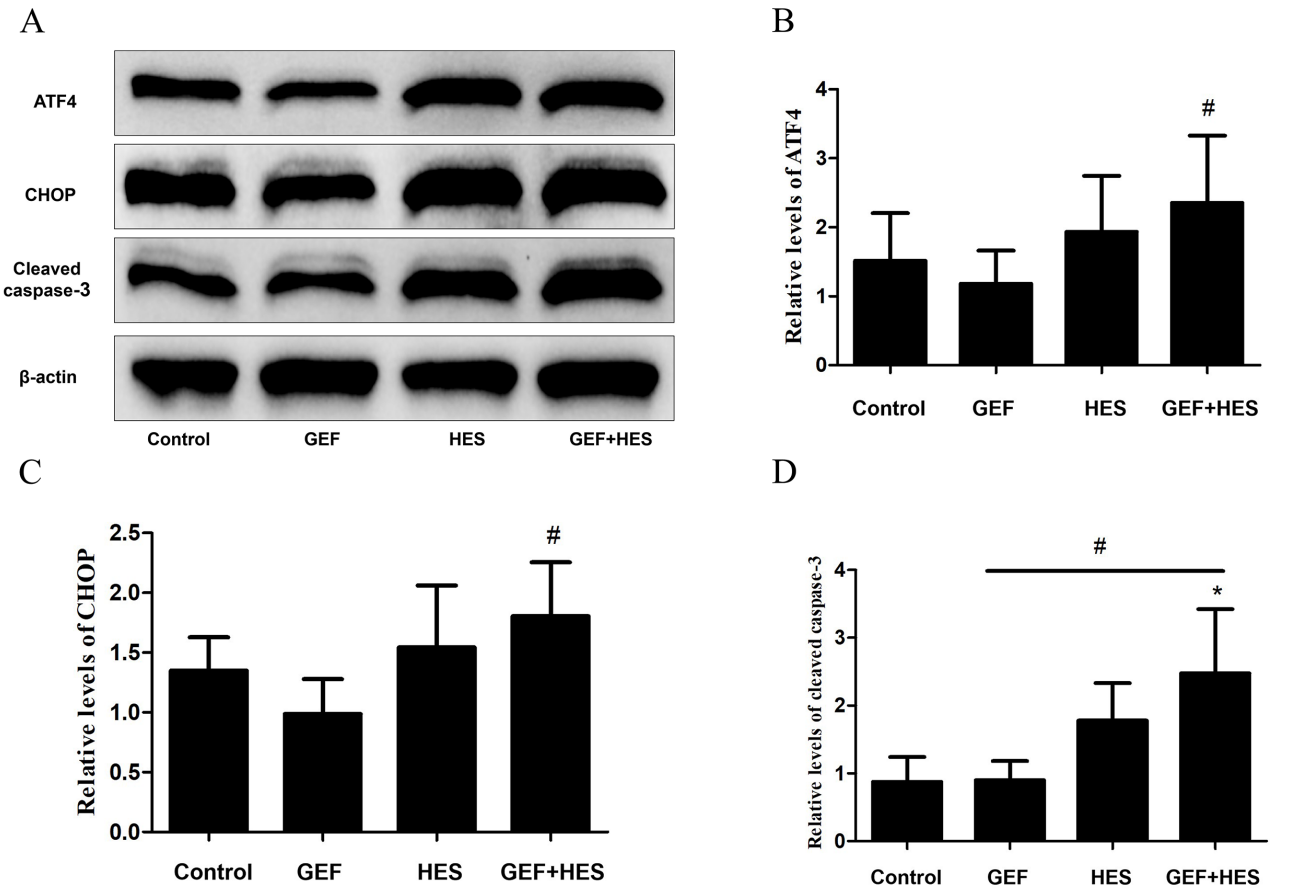

Fig. 5. Effects of HES and GEF on the protein expression of endoplasmic reticulum stress-related markers and cleaved caspase-3 in A549 cells. (A) Representative Western blot images showing protein bands for ATF4, CHOP, cleaved caspase-3, and β-actin (loading control). (B) Densitometric quantification of ATF4 expression normalized to β-actin. (C) Densitometric quantification of CHOP expression normalized to β-actin. (D) Densitometric quantification of cleaved caspase-3 expression normalized to β-actin. Cells were treated with control, GEF, HES, and GEF + HES for 48 h. Data are presented as the mean ± SD from three independent experiments. $^{*}p < 0.05$ indicates a significant difference compared to the control group; $^{\#}p < 0.05$ indicates a significant difference compared to the single-drug treatment group. ATF4, activating transcription factor 4; CHOP, C/EBP homologous protein.

the HES/GEF combination significantly inhibited A549 cell proliferation and migration, while effectively inducing apoptosis. These findings were further corroborated *in vivo* using a nude mouse xenograft model, where the combination regimen exerted enhanced inhibition of tumor growth. Our results are consistent with previous reports in other tumor types. For instance, in a breast cancer model, HES combined with doxorubicin significantly inhibited tumor growth in mice. This was accompanied by elevated IFN-γ levels, decreased expression of proliferation and angiogenesis markers Ki-67 and vascular endothelial growth factor (VEGF), and increased E-cadherin expression, indicating synergistic enhancement of chemotherapeutic efficacy [28]. In prostate cancer, HES suppressed cell proliferation and enhanced the anticancer activity of cisplatin by inducing oxidative stress, disrupting calcium homeostasis, triggering mitochondrial depolarization, and activating ERS [29]. Recent studies also showed that HES combined with bleomycin exerts enhanced anti-proliferative and pro-apoptotic effects in A549 cells [30]. Moreover, HES potentiated the pro-apoptotic and anti-inflammatory activities of adriamycin in a cervical cancer model [31]. Collectively, these lines of evidence broadly support the potential of HES as a sensitizer in combination therapy. The present study extends this knowledge by demonstrating, an enhanced interaction between HES and the EGFR-TKI GEF in NSCLC. Additionally, we provide preliminary insights into the underlying pathway.

At the mechanistic level, under persistent ERS, the PERK-eIF2α-ATF4-CHOP axis serves as a core pro-apoptotic branch of the UPR and is increasingly recognized as a promising therapeutic target in NSCLC. Activation of this pathway ultimately leads to cleavage and activation of the executioner caspase-3, which initiates the irreversible proteolytic cascade of apoptosis. Several natural compounds have been shown to exert antitumor effects

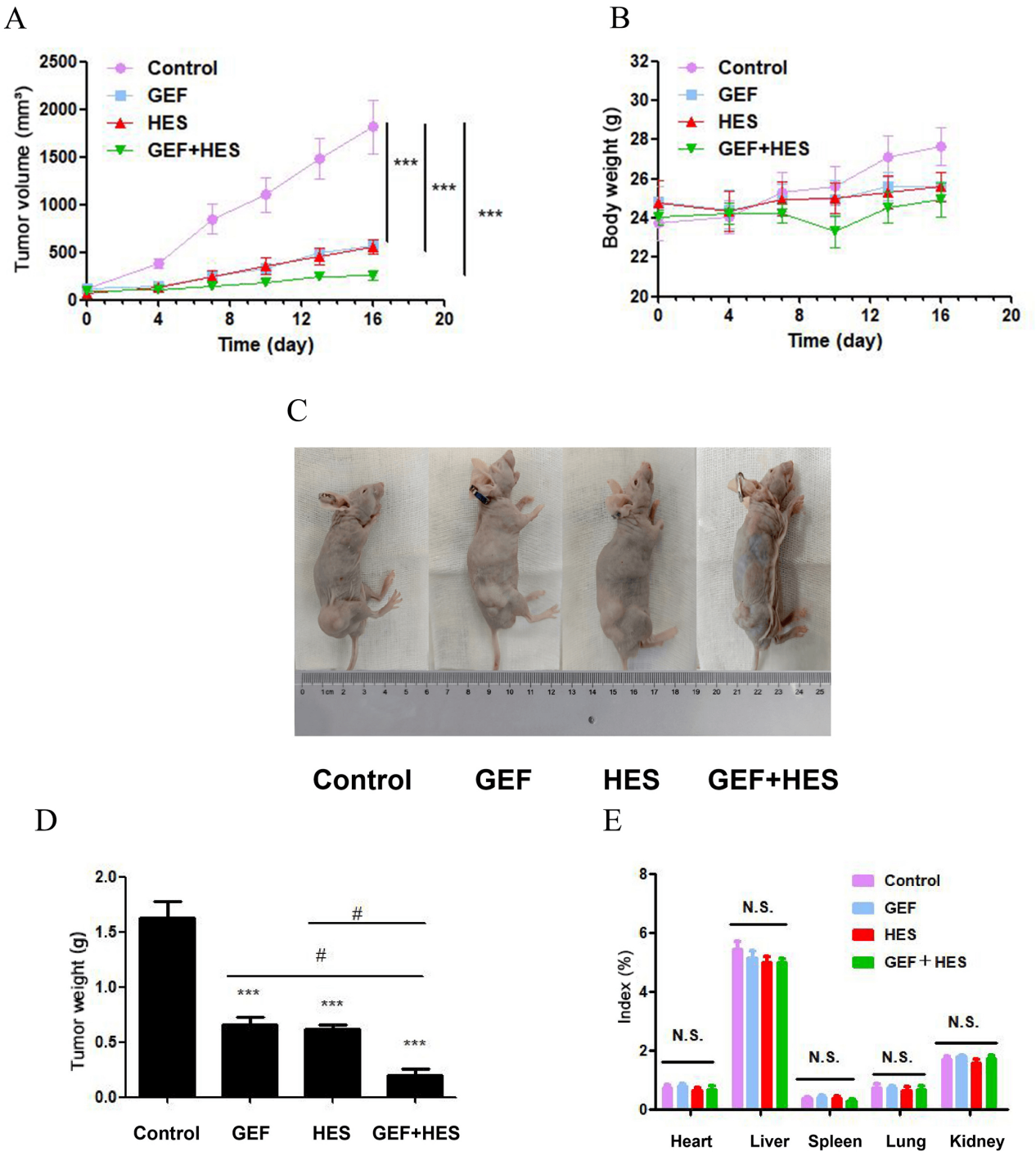

Fig. 6. The inhibitory effect of HES and GEF on the growth of xenograft tumors in nude mice. (A) Xenograft tumor growth curves. (B) Weight changes in nude mice across groups. (C) Gross view of xenograft tumors in nude mice. (D) Tumor weights in each group. (E) Organ indices of heart, liver, spleen, lung, and kidney. n = 6; $^{\#}p < 0.05$ indicates a significant difference; $^{***}p < 0.001$ denotes a highly significant difference; N.S. indicates not statistically significant.

in NSCLC through the ATF4/CHOP/caspase-3-dependent apoptotic pathway, suggesting that pharmacological activation of ERS-mediated apoptosis is a feasible therapeutic strategy. In the present study, combined HES and GEF treatment significantly upregulated ATF4 and CHOP expression, accompanied by cleaved caspase-3 activation. These results indicate that ERS-mediated apoptosis is one of the key molecular events underpinning the enhanced antitumor effect of HES and GEF. This notion is further supported by the work of Xu et al. [32], who found that the

Nrf2 inhibitor ML385 combined with celastrol not only further reduced lung cancer cell viability and significantly elevated ROS levels, but also potentiated celastrol-induced ATF4/CHOP-dependent ERS through the suppression of heme oxygenase-1 (HO-1) and glutamate–cysteine ligase catalytic subunit (GCLC) expression.

Regarding safety, the combined HES and GEF regimen did not significantly affect body weight or major organ indices (heart, liver, spleen, lung, kidney) in nude mice. Although no overt systemic toxicity was observed at the tested doses, future preclinical studies should incorporate comprehensive ADMET (absorption, distribution, metabolism, excretion, and toxicity) evaluations, including pharmacokinetic profiling and assessment of markers for hepatic function, such as alanine aminotransferase (ALT) and aspartate aminotransferase (AST), and renal function, such as blood urea nitrogen (BUN) and creatinine. This should enable more systematic and objective validation of the safety profile of the HES and GEF combination, thereby providing robust data to support its translational potential.

Limitations

Although the present study provides preliminary evidence for the enhanced antitumor effect of HES combined with GEF in NSCLC and its activation of the ERS pathway, several limitations should be acknowledged and warrant further investigation. First, at the mechanistic level, while we observed upregulation of the ATF4/CHOP/caspase-3 axis, we did not employ specific pharmacological inhibitors or gene silencing approaches (e.g., siRNA) to functionally intervene in these pathway components. Therefore, our current conclusions are primarily based on correlative evidence and do not establish direct causality. Moreover, the individual contributions of the three upstream UPR sensors (PERK, IRE1α, and ATF6) to the effects of this combination remain to be determined, as well as potential cross-regulation among them. Future studies should incorporate relevant pathway inhibitors and knockout models to systematically dissect the precise molecular switches through which the HES and GEF combination activates ERS and the downstream apoptotic signaling network. Second, the xenograft model was established in immunodeficient nude mice lacking T-cell-mediated adaptive immune responses, thus precluding evaluation of potential immunomodulatory effects of the combination therapy. Furthermore, the subcutaneous ectopic model does not fully recapitulate the native tumor microenvironment of orthotopic lung cancer, including tumor-stromal cell interactions and the pulmonary niche. Consequently, it will be essential in future studies to validate the comprehensive efficacy and immune-related mechanisms of this combination in immunocompetent orthotopic mouse models. Third, the relatively short treatment duration (16 days) and modest sample size (n = 6 per group) limit our ability to adequately assess the long-term safety and durability of the antitumor response. Subsequent studies should extend the observation period, increase the sample size, and incorporate NSCLC cell lines with diverse genetic backgrounds (e.g., EGFR-mutant and TKI-resistant lines) to enhance the generalizability and clinical relevance of the findings.

In summary, this work provides a valuable preliminary foundation for the use of HES in combination with GEF for NSCLC treatment. However, more refined mechanistic dissection, more clinically relevant model systems, and longer-term safety observations are required to strengthen the basis for further translational research.

Despite these limitations, the present findings have important translational implications. The use of a dietary flavonoid like HES as a chemosensitizer offers a low-cost, low-toxicity adjunctive strategy that could potentially be integrated into current EGFR-TKI-based regimens. Given the excellent safety profile of HES in humans as a food-derived compound, this combination warrants further investigation in preclinical models that more closely recapitulate the clinical setting, with the ultimate goal of improving outcomes for NSCLC patients with intrinsic TKI resistance.

5. Conclusion

This study demonstrates that the combination of hesperidin and gefitinib exerts enhanced antiproliferative and pro-apoptotic effects in human NSCLC A549 cells and a nude mouse xenograft model. Furthermore, this effect appears to be at least partially mediated through activation of the endoplasmic reticulum stress signaling pathway. The combination regimen exhibited favorable tolerability *in vivo*, thus offering a novel, natural product-based candidate strategy to overcome intrinsic resistance to EGFR-TKIs and optimize targeted therapy for NSCLC. Further preclinical and clinical exploration of this combination treatment is warranted.

Availability of Data and Materials

The datasets used and analyzed during the current study are available from the corresponding author upon reasonable request.

Author Contributions

JP and YW designed the overall study. YW and TL guided the experimental implementation. TL and YL conducted the experiments, analyzed the data, and drafted the manuscript. JY assisted in literature search and data collection. DL secured funding, participated in the conception of the study, provided scientific guidance, and interpreted the results for the study. All authors contributed to editorial changes in the manuscript. All authors read and approved the final manuscript. All authors have participated sufficiently in the work and agreed to be accountable for all aspects of the work.

Ethics Approval and Consent to Participate

This experiment was conducted in accordance with the regulations of the Biomedical Ethics Committee of Chongqing Three Gorges Medical College. The project has received ethical approval (Approval No.: SXYZ-A-2404-0011), and the experimental procedures strictly followed the relevant regulations of Chongqing Three Gorges Medical College concerning animal welfare and were carried out in accordance with the National Institutes of Health (NIH) Guide for the Care and Use of Laboratory Animals and the ARRIVE guidelines.

Acknowledgment

The authors wish to express their sincere appreciation to the Chongqing Key Laboratory of Development and Utilization of Genuine Medicinal Materials in the Three Gorges Reservoir Area for its support. The Graphical Abstract was created using MedPeer software.

Funding

This research was supported by the following grants: the Science and Technology Research Project of Chongqing Education Commission (Award Numbers: KJQN202402730); the Major Natural Science Project of Chongqing Three Gorges Medical College (Award Number: XJ2022003103); and a General Project from Chongqing Three Gorges Medical College (Award Number: XJ2022002205).

Conflicts of Interest

The authors declare no conflicts of interest.

Declaration of AI and AI-Assisted Technologies in the Writing Process

In the process of this research, the authors utilized the AI language model GPT-4 to assist in refining the linguistic expression, identifying grammatical inaccuracies, and enhancing the clarity and flow of the draft manuscript. It is important to note that the authors meticulously reviewed and revised all AI-generated suggestions, and they affirm the scientific integrity of the work and accept complete accountability for its content.

Supplementary Material

Supplementary material associated with this article can be found, in the online version, at https://doi.org/10.31083/IJP53817.

References

[1] Bray F, Laversanne M, Sung H, Ferlay J, Siegel RL, Soerjomataram I, et al. Global cancer statistics 2022: GLOBOCAN estimates of incidence and mortality worldwide for 36 cancers in 185 countries. CA: a Cancer Journal for Clinicians. 2024; 74: 229–263. https://doi.org/10.3322/caac.21834

[2] Zappa C, Mousa SA. Non-small cell lung cancer: current treatment and future advances. Translational Lung Cancer Research. 2016; 5: 288–300. https://doi.org/10.21037/tlcr.2016.06.07

[3] Bade BC, Dela Cruz CS. Lung Cancer 2020: Epidemiology, Etiology, and Prevention. Clinics in Chest Medicine. 2020; 41: 1–24. https://doi.org/10.1016/j.ccm.2019.10.001

[4] Shivika, Sharma M, Bajpai A, Dar ZA, Singh R, Bansal R. Therapeutic dominance of tyrosine kinase inhibitors in non-small cell lung cancer (NSCLC). Bioorganic Chemistry. 2025; 163: 108660. https://doi.org/10.1016/j.bioorg.2025.108660

[5] Dmitrieva AM, Kocak IG, Meder L. Aberrations in the glycosylation of receptor tyrosine kinases: A focus on lung adenocarcinoma. CytoJournal. 2025; 22: 62. https://doi.org/10.25259/Cytojournal_21_2025

[6] Cho BC, Ahn MJ, Kang JH, Soo RA, Reungwetwattana T, Yang JCH, et al. Lazertinib Versus Gefitinib as First-Line Treatment in Patients With *EGFR*-Mutated Advanced Non-Small-Cell Lung Cancer: Results From LASER301. Journal of Clinical Oncology : Official Journal of the American Society of Clinical Oncology. 2023; 41: 4208–4217. https://doi.org/10.1200/JCO.23.00515

[7] Tian Z, Cen L, Wei F, Dong J, Huang Y, Han Y, et al. EGFR mutations in non-small cell lung cancer: Classification, characteristics and resistance to third-generation EGFR-tyrosine kinase inhibitors (Review). Oncology Letters. 2025; 30: 375. https://doi.org/10.3892/ol.2025.15121

[8] Antrim LJ, Malhotra J. Treating EGFR-mutant nonsmall cell lung cancer is no longer a one-size-fits-all approach. CA: a Cancer Journal for Clinicians. 2025; 75: 373–375. https://doi.org/10.3322/caac.70027

[9] Alrumaihi F, Rahmani AH, Prabhu SV, Kumar V, Anwar S. The Role of Plant-Derived Natural Products as a Regulator of the Tyrosine Kinase Pathway in the Management of Lung Cancer. Current Issues in Molecular Biology. 2025; 47: 498. https://doi.org/10.3390/cimb47070498

[10] Han D, Gong H, Wei Y, Xu Y, Zhou X, Wang Z, et al. Hesperidin inhibits lung fibroblast senescence via IL-6/STAT3 signaling pathway to suppress pulmonary fibrosis. Phytomedicine : International Journal of Phytotherapy and Phytopharmacology. 2023; 112: 154680. https://doi.org/10.1016/j.phymed.2023.154680

[11] Kim HJ, Jin BR, An HJ. Hesperidin ameliorates benign prostatic hyperplasia by attenuating cell proliferation, inflammatory response, and epithelial-mesenchymal transition via the TGF-β1/Smad signaling pathway. Biomedicine & Pharmacotherapy = Biomedecine & Pharmacotherapie. 2023; 160: 114389. https://doi.org/10.1016/j.biopha.2023.114389

[12] Wang X, Nie T, Li A, Ma J. Hesperidin mitigated deoxynivalenol-induced liver injury by inhibiting ROS/P53/ PGC-1α-mediated disruption of mitochondrial dynamics and PANoptosis. Phytomedicine : International Journal of Phytotherapy and Phytopharmacology. 2025; 142: 156747. https://doi.org/10.1016/j.phymed.2025.156747

[13] Guan Y, Ruan J, Tan P, Qian S, Zhou S, Zhang A, et al. Hesperidin alleviates endothelial cell inflammation and apoptosis of Kawasaki disease through inhibiting the TLR4/IκBα/NF-κB pathway. Chemico-biological Interactions. 2025; 411: 111445. https://doi.org/10.1016/j.cbi.2025.111445

[14] Syed AA, Reza MI, Yadav H, Gayen JR. Hesperidin inhibits NOX4 mediated oxidative stress and inflammation by upregulating SIRT1 in experimental diabetic neuropathy. Experimental Gerontology. 2023; 172: 112064. https://doi.org/10.1016/j.exger.2022.112064

[15] Xu H, Yu S, Lin C, Dong D, Xiao J, Ye Y, et al. Roles of flavonoids in ischemic heart disease: Cardioprotective effects and mechanisms against myocardial ischemia and reperfusion injury. Phytomedicine : International Journal of Phytotherapy and Phytopharmacology. 2024; 126: 155409. https://doi.org/10.1016/j.phymed.2024.155409

[16] Li X, Huang W, Tan R, Xu C, Chen X, Li S, et al. The benefits of hesperidin in central nervous system disorders, based on the neuroprotective effect. Biomedicine & Pharmacotherapy = Biomedecine & Pharmacotherapie. 2023; 159: 114222. https://doi.org/10.1016/j.biopha.2023.114222

[17] Madureira MB, Concato VM, Cruz EMS, Bitencourt de Morais JM, Inoue FSR, Concimo Santos N, et al. Naringenin and Hesperidin as Promising Alternatives for Prevention and Co-Adjuvant Therapy for Breast Cancer. Antioxidants (Basel, Switzerland). 2023; 12: 586. https://doi.org/10.3390/antiox12030586

[18] Yao Y, Lin M, Liu Z, Liu M, Zhang S, Zhang Y. Hesperidin Inhibits Lung Cancer *In Vitro* and *In Vivo* Through PinX1. Frontiers in Pharmacology. 2022; 13: 918665. https://doi.org/10.3389/fphar.2022.918665

[19] Gou W, Luo N, Wei H, Wu H, Yu X, Duan Y, et al. Ursolic acid derivative UA232 evokes apoptosis of lung cancer cells induced by endoplasmic reticulum stress. Pharmaceutical Biology. 2020; 58: 707–715. https://doi.org/10.1080/13880209.2020.1794013

[20] Im JY, Kim SJ, Park JL, Han TH, Kim WI, Kim I, et al. CYB5R3 functions as a tumor suppressor by inducing ER stress-mediated apoptosis in lung cancer cells via the PERK-ATF4 and IRE1α-JNK pathways. Experimental & Molecular Medicine. 2024; 56: 235–249. https://doi.org/10.1038/s12276-024-01155-9

[21] Xu Z, Huang X, Su Q, Wang Q, Liu L, Shen Y, et al. Flemiphilippinin A induces paraptosis in lung cancer cells via c-Myc-driven endoplasmic reticulum stress and CHOP-mediated mitochondrial dysfunction. Phytomedicine : International Journal of Phytotherapy and Phytopharmacology. 2025; 146: 157098. https://doi.org/10.1016/j.phymed.2025.157098

[22] Xie Q, He Z, Tan L, Li M, Zhuang M, Liu C, et al. Hesperetin induces apoptosis in lung squamous carcinoma cells via G_2/M cycle arrest, inhibition of the Notch1 pathway and activation of endoplasmic reticulum stress. International Journal of Molecular Medicine. 2025; 55: 77. https://doi.org/10.3892/ijmm.2025.5518

[23] Yan WY, Cai J, Wang JN, Gong YS, Ding XB. Co-treatment of betulin and gefitinib is effective against EGFR wild-type/KRAS-mutant non-small cell lung cancer by inducing ferroptosis. Neoplasma, 2022; 69: 648-656. https://doi.org/10.4149/neo_2022_211103N1568

[24] Fu B, Dou X, Zou M, Lu H, Wang K, Liu Q, et al. Anticancer Effects of Amlodipine Alone or in Combination With Gefitinib in Non-Small Cell Lung Cancer. Frontiers in Pharmacology. 2022; 13: 902305. https://doi.org/10.3389/fphar.2022.902305

[25] Zhu L, Shi J, Mu M, Chen Z, Zhao C, Li X, et al. Naringin Inhibits the Proliferation, Migration, Invasion and Epithelial-to-Mesenchymal Transition of Gastric Cancer Cells via the PI3K/AKT Signaling Pathway. Alternative Therapies in Health and Medicine. 2023; 29: 191–197.

[26] Huang X, Sun J, Sun J. Combined Treatment with JFKD and Gefitinib Overcomes Drug Resistance in Non-Small Cell Lung Cancer. Current Pharmaceutical Biotechnology. 2021; 22: 389–399. https://doi.org/10.2174/1389201021999200819105209

[27] Zeng W, Xia L. Mechanistic of Artemisinin Extracts Modulating Cisplatin Resistance in Lung Cancer A549/DDP Cells via the PI3K/Akt Pathway. International Journal of Pharmacology. 2025; 21: 217-230. https://doi.org/10.3923/ijp.2025.217.230

[28] Shakiba E, Bazi A, Ghasemi H, Eshaghi-Gorji R, Mehdipour SA, Nikfar B, et al. Hesperidin suppressed metastasis, angiogenesis and tumour growth in Balb/c mice model of breast cancer. Journal of Cellular and Molecular Medicine. 2023; 27: 2756–2769. https://doi.org/10.1111/jcmm.17902

[29] Jeong SA, Yang C, Song J, Song G, Jeong W, Lim W. Hesperidin Suppresses the Proliferation of Prostate Cancer Cells by Inducing Oxidative Stress and Disrupting Ca^{2+} Homeostasis. Antioxidants (Basel, Switzerland). 2022; 11: 1633. https://doi.org/10.3390/antiox11091633

[30] Erdogan MK, Ozer G. Synergistic Anticancer Effects of Bleomycin and Hesperidin Combination on A549 Non-Small Cell Lung Cancer Cells: Antiproliferative, Apoptotic, Anti-Angiogenic, and Autophagic Insights. Pharmaceuticals (Basel, Switzerland). 2025; 18: 254. https://doi.org/10.3390/ph18020254

[31] Özdemir İ, Afşin Y, Tuncer MC, Öztürk Ş. Combined Hesperidin and Doxorubicin Treatment Induces Apoptosis and Modulates Inflammatory Cytokines in HeLa Cervical Cancer Cells. International Journal of Molecular Sciences. 2025; 26: 8753. https://doi.org/10.3390/ijms26178753

[32] Xu C, Chen Y, Zhou Z, Yan Y, Fu W, Zou P, et al. ML385, an Nrf2 Inhibitor, Synergically Enhanced Celastrol Triggered Endoplasmic Reticulum Stress in Lung Cancer Cells. ACS Omega. 2024; 9: 43697–43705. https://doi.org/10.1021/acsomega.4c06152